DOI 10.1007/s00289-017-2124-x

Polyurethane porous scaffolds (PPS) for soft tissue regenerative medicine applications

J. Kucińska-Lipka[1] · I. Gubanska[1] · M. Pokrywczynska[2] · H. Ciesliński[3] · N. Filipowicz[3] · T. Drewa[2,4] · H. Janik

Abstract Tissue engineering requires suitable polymeric scaffolds, which act as a physical support for regenerated tissue. A promising candidate might be polyurethane (PUR) scaffold, due to the ease of the PUR properties design, which can be adjusted directly to the intended purpose. In this study, we report a successful fabrication of porous polyurethane scaffolds (PPS) using solvent casting/particulate leaching technique combined with thermally induced phase separation. The obtained PPS had comparable chemical structure to native PUR, which was confirmed by FTIR and HNMR analyses. The performed DSC study determined a similar T_g of the obtained PPS to native PUR (−38 °C). The analysis of TEM micrographs revealed that PPS had a homogenous structure. The studied PPS interactions with canola oil, distilled water, saline solution and phosphate-buffered saline after 3 months of incubation revealed that these materials have stable character in these media. The significant decrease of contact angle from 68° for native PUR to 54° for PPS was noted, as well as the decrease of mechanical properties ($T_{Sb} \sim 1$ MPa and $\varepsilon_b \sim 95\%$ of PPS were comparable to the native aorta tissue of $T_{Sb} \sim 0.3$–0.8 MPa and $\varepsilon_b \sim 50$–100%). Through SEM analysis, the morphology of the PPS was determined: the porosity was 87% and the pore sizes in the range of 98–492 μm. The biological studies revealed that the obtained PPS are sensitive to

[1] Department of Polymers Technology, Faculty of Chemistry, Gdank University of Technology, Narutowicza St. 11/12, 80-233 Gdańsk, Poland

[2] Chair of Regenerative Medicine, Ludwik Rydygier Medical College in Bydgoszcz, Nicolaus Copernicus University in Torun, Karlowicza 24 Street, 85-092 Bydgoszcz, Poland

[3] Department of Microbiology, Faculty of Chemistry, Gdansk University of Technology, Narutowicza St. 11/12, 80-233 Gdańsk, Poland

[4] Department of Urology, Nicolaus Copernicus Hospital, Batory 17-19 Street, 87-100 Toruń, Poland

microorganisms such as *Staphylococcus aureus*, *Pseudomonas aeruginosa* and *Escherichia coli* and that they are biocompatible with the 3T3 NIH cell line. In summary, the obtained PPS scaffolds may be a suitable material for soft tissue engineering like blood vessels.

Keywords Polyurethane · Scaffold · Regenerative medicine · Tissue engineering · Porosity · Blood vessel

Introduction

Tissue engineering has been an expanding field of regenerative medicine. Since 10 years, it has served novel solutions for regeneration of tissues and organs of the human body. The aim of tissue engineering is to restore, maintain, or improve tissue functions, which are defective or have been lost in some circumstances. Tissue restoration may be carried out by developing biological substitutes or reconstructing tissues with the use of natural or synthetic scaffolds [1].

The design and fabrication of scaffolds is a major concern of biomaterials and tissue engineering research [2]. Scaffolds play a unique role in tissue regeneration and repair. They are defined as three-dimensional porous solid biomaterials designed to: promote cell–biomaterial interactions, cell adhesion, and ECM deposition; permit sufficient transport of gases, nutrients, and regulatory factors to allow cell survival; proliferation, and differentiation; biodegrade at a controllable rate that approximates the rate of tissue regeneration under the culture conditions of interest; and provoke a minimal degree of inflammation or toxicity in vivo [3]. The design of scaffolds with the optimal characteristic such as suitable mechanical properties, rate of degradation, porosity, and microstructure are more readily and reproducibly controlled in scaffolds produced with the use of synthetic biomaterials than in natural ones [4].

Biomaterials are commonly used as implants in the form of sutures, bone plates, joint replacements, ligaments, vascular grafts, heart valves, intraocular lenses, dental implants, and medical devices such as pacemakers, biosensors, and so forth [5, 6]. Synthetic or natural biomaterials play a critical role in the porous scaffold fabrication by acting as synthetic frameworks for cells. Both synthetic and natural polymers have been widely used as biomaterials for the fabrication of medical devices and tissue engineering scaffolds [7, 8].

Polymeric scaffolds possess unique properties such as high surface-to-volume ratio, high porosity with very small pore size, suitable biodegradation rate, and mechanical properties. Polymeric scaffolds can provide the advantages of biocompatibility, versatility of chemistry, and the biological properties, which are significant in the regenerative medicine of tissues. Properly designed polymeric scaffolds may guide the restoration of structure and function of damaged or diseased tissues. Synthetic polymers have also major advantage over other materials, which is the fact that they can be produced in large uniform quantities and have a long shelf time. They exhibit predictable and reproducible mechanical and physical properties such as tensile strength, elastic modulus, and degradation rate [9]. Many

commercially available synthetic polymers show physicochemical and mechanical properties comparable to those of native tissues. Synthetic polymers, such as polylactide (PLA), polyglicolide (PGA), and poly(lactide-co-glicolide) (PLGA) copolymers are among the most commonly used synthetic polymers in tissue engineering [10]. In recent years, extensively studied materials for tissue engineering applications are polyurethanes (PURs) [11, 12]. Biostable PURs have been used as biomedical devices from the 1960s. Recent studies are mainly concerned about biodegradable PURs, which have been investigated for applications in tissue engineering [13]. In contrast to the biostable implants, these PUR biomaterials are designed to undergo controlled degradation in vivo and to promote ingrowth of new tissue [14].

Since 1980, researchers have developed many novel techniques to shape polymers into complex architectures that exhibit the desired properties for specific tissue engineering applications. These fabrication techniques result in reproducible scaffolds for the regeneration of specific tissues [1]. Tissue engineered scaffolds can be fabricated into biodegradable porous scaffolds by using a variety of techniques, including thermally induced phase separation (TIPS), solvent casting/particulate leaching (SC/PL), wet spinning, electrospinning [15], and carbon dioxide foaming. Most techniques involve the application of heat and/or pressure to the polymer or dissolving it in an organic solvent to mold the material into its desired shape. Depending on the choice of solvent and phase separating conditions, the foams can be controlled to form either random or oriented pore architectures [16]. The proper selection of scaffold fabrication method provides a scaffold of the desired porosity, morphology, and anisotropy [14, 17]. Usually, fabricated scaffolds are in the shape of meshes, fibers, foams, and sponges. This is due to the fact that such microporous scaffolds promote uniform cell distribution, diffusion of nutrients, and the growth of organized cell communities [18]. The appropriate scaffold fabrication technique must be selected to meet the requirements for the specific type of tissue that it will regenerate [19]. For enhanced control over porosity and pore diameter as compared to most fabrication methods, a solvent casting and particulate leaching technique was developed. To achieve directed tissue regeneration, the chemistry and physicochemical properties of the tissue scaffolds have to be well defined. Successful 3D scaffolds possess suitable: (1) external geometry (e.g., macro- and microstructure as well as interconnectivity), (2) surface properties (e.g., surface energy, chemistry, charge, surface area), (3) porosity and pore size, (4) interface adherence and biocompatibility, (5) degradation characterization (e.g., biodegradation), (6) mechanical properties (e.g., compressive and tensile strength) [1]. Developing scaffolds that mimic the architecture of tissue at the nanoscale is one of the most important challenges in the field of tissue engineering [20]. Polymeric scaffolds show excellent potential with mechanical properties and with a wide range of degradation, the qualities which are essential for a range of tissue engineering applications [21].

In this study, we synthesized polyurethanes (PUR) with the use of oligomeric α,ω-dihydroxy(ethylene–butylene adipate) (dHEBA), cycloaliphatic 4,4-methylene bis(cyclohexyl isocyanate) (HMDI), and 1,4-butanediol as a chain extender in the microwave reactor. The obtained materials were further successfully fabricated

into porous polyurethane scaffolds (PPS) with the use of solvent casting particulate leaching (SC/PL) technique combined with thermally induced phase separation (TIPS). The PPS had preserved chemical structure of native PUR, which was evaluated by the FTIR and HNMR spectra analysis. The DSC study determined that the native PUR and fabricated PPS had similar T_g (−38 °C). The analysis of TEM micrographs revealed that PPS had a homogenous structure. The studied PPS interactions with canola oil, distilled water, saline solution, and phosphate-buffered saline (PBS) after 3 months of incubation revealed that these materials did not undergo degradation and were stable, which is desired for tissue engineering purpose. The significant decrease of contact angle from 68° for native PUR to 54° for PPS was noted, as well as the decrease of mechanical properties ($T_{Sb} \sim 1$ MPa and $\varepsilon_b \sim 95\%$ of PPS were comparable to the native aorta tissue of $T_{Sb} \sim 0.3$-0.8 MPa and $\varepsilon_b \sim 50$–100%). Thus, the processing of native PUR into the PPS had significant impact on these properties. Through SEM analysis, the morphology of the PPS was characterized. The porosity was of 87% and pore sizes in the range of 98–329 µm. Biological studies revealed that the obtained PPS are sensitive to microorganisms such as *Staphylococcus aureus*, *Pseudomonas aeruginosa*, and *Escherichia coli* and that they are biocompatible with 3T3 NIH cell line. In summary, the obtained PPS scaffolds may be suitable materials for soft tissue engineering like blood vessels.

Materials and methods

Native polyurethane synthesis (PUR)

Native PURs were obtained by using oligomeric α,ω-dihydroxy(ethylene–butylene adipate) (dHEBA) polyester (trade name Polios 55/20; Purinova, Poland), 1,4-butanediol (BDO) chain extender and diisocyanate of cycloaliphatic structure (4,4-methylene bis(cyclohexyl isocyanate, HMDI, Sigma Aldrich, Poland), which is a mixture of isomers (cis–cis, trans–trans, trans–cis, Fig. 1).

The in-bulk synthesis of PUR was performed by a two-step polymerization procedure [23]. Briefly, the urethane prepolymer of 8% free isocyanate groups was obtained with the use of Polios 55/20 and HMDI. The urethane prepolymer reaction was carried out at 80 °C for 60 min, under constant mixing, in the microwave reactor (MR, Ertec model NOVA 09) to overcome the necessity of the catalyst application. The power of the microwave reactor was set at 90% of its maximum power (max. power 750 W, field frequency of 2.45 GHz). Then, the chain extender BDO was added to the system to obtain PUR with optimal mechanical properties [23]. The urethane prepolymer reaction with the BDO

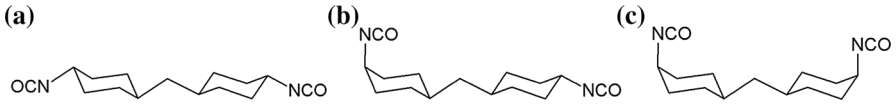

Fig. 1 Isomers of HMDI: **a** trans–trans, **b** cis–trans, **c** cis–cis [20]

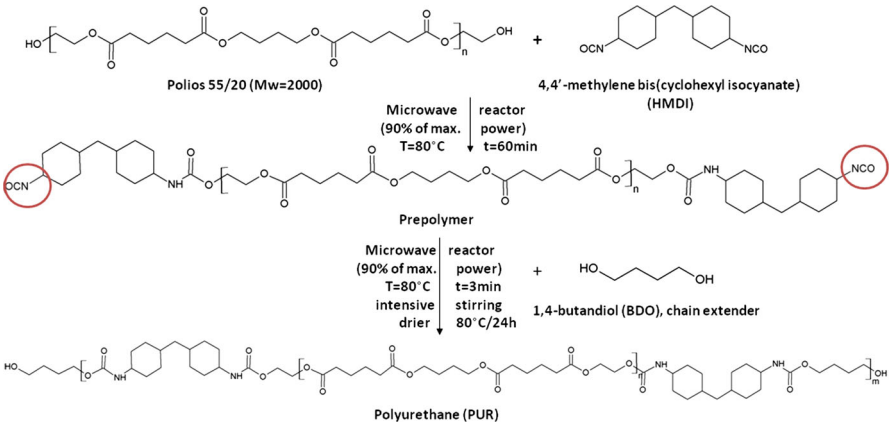

Fig. 2 Scheme of native PUR synthesis

chain extender was subjected to intensive stirring at 80 °C for 3 min to form PUR. The obtained PUR material was then left in a dryer at 80 °C for 24 h to complete the reaction. The scheme of the PUR synthesis is presented in Fig. 2.

Porous polyurethane scaffolds (PPS) fabrication

To obtain PPS, solvent casting/particulate leaching (SC/PL) technique combined with thermally induced phase separation (TIPS) was used. PUR was dissolved in 1,4-dioxane (POCH, Poland) at a concentration of 20% wt/v. Then, sodium chloride (NaCl), of crystals size in the range of 0.6–0.4 μm, was added to the polyurethane solution until complete saturation of the solution occurred. The formulated PUR salt-saturated solution was transferred into the stainless steel mold of the size 2.5 × 2.5 × 2.5 cm and placed at −20 °C for 24 h to direct the solvent crystallization and to fabricate scaffolds of local anisotropy where the porosity of scaffolds is of controlled pore size and porosity [24–26]. Then PPS were removed from the mold and immersed in warm (40–50 °C) bidistilled water, where for 7 days the NaCl crystals were washed out. Water was changed twice a day. Finally, the samples of PPS were dried at 60 °C for 24 h. The scheme of PPS fabrication is presented in Fig. 3.

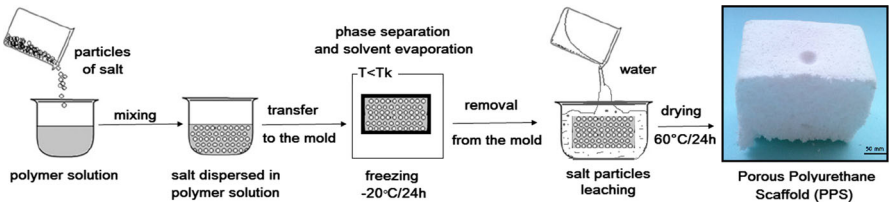

Fig. 3 Scheme of PPS fabrication

Fourier Transform infrared spectroscopy (FTIR)

The FTIR of the fabricated PPS and native PUR was performed with an FTIR Nicolet 8700 Spectrometer to determine the influence of the processing technique on the chemical composition of the obtained materials. The studied spectral range was from 4000 to 500 cm^{-1}, averaging 254 scans per sample with a resolution of 4 cm^{-1}.

Proton nuclear magnetic resonance (^{1}HNMR)

The ^{1}HNMR spectra of fabricated PPS and native PUR were obtained by 500 MHz Varian Spectrometer Unity 500 Plus using deuterated dimethylsulfoxide (DMSO) as PUR solvent. ^{1}HNMR was used to determine the possible influence of the processing technique on the chemical structure of the obtained PUR materials.

Differential scanning calorimetry (DSC) and transmission electron microscopy (TEM)

DSC was performed on a NETZSCH DSC 204 F1 Phoenix apparatus. Fabricated PPS and native PUR samples, of 10-mg mass, were studied at a temperature range of −30 to 250 °C and under N_2 atmosphere with a heating rate of the sample equal to 20 °C/min. The results of DSC analysis determined the melting point (T_m) and the glass transition temperature (T_g) of fabricated PPS and native PUR materials.

TEM was performed to complement the DSC analysis. Fabricated PPS and native PUR samples were studied with the use of Tesla BS 500 (accelerating voltage 60 kV) transmission electron microscope. To study micro and nanostructure, thin films technique was used. Fabricated PPS or native PUR was dissolved in 4,4′-dimethylformamide (DMF) solvent for 24 h at 60 °C. Then the resulting solution was transferred to a TEM grid, coated with thin carbon film and left to dry under vacuum for 24 h. TEM was performed at a magnification of 3000×. TEM micrographs were fixed on photographic films (type IMAGO-EM23 efke scope) and then analyzed [27].

Interactions with canola oil, saline, distilled water, and phosphate-buffered saline

Fabricated PPS and native PUR were cut into six samples of a 1 cm^2 area and then dried and weighed in a Thermobalance (RADWAG MAX50/SX) set at 60 °C. The prepared samples were placed in multiwell testing plates filled with canola oil, distilled water, saline, or phosphate-buffered saline (PBS). Studies of biomedical material interactions with different media are common in case of medical-grade polymers [28]. Canola oil absorptivity may be used to determine the in situ behavior of the biomaterials according to the lipids present in the living body [29]. The exposure of biomaterials to lipids may lead, in in vivo conditions, to swelling and degradation in otherwise stable biomaterials [30]. Furthermore, drugs delivered to the body, encapsulated in a biodegradable polymer, are often introduced to the

system as a lipid emulsion [31]. Samples were incubated in a selected media at room temperature. Changes of samples' weight were examined after 1 day of incubation for canola oil medium; after 1, 3, 7, 14 days, and 1, 2, and 3 months for distilled water, saline, and PBS [28]. The measurement procedure was as follows: samples were taken from the container and placed between paper towels to reduce the excess of medium used in the test. The samples were then placed in a thermobalance (set at 60 °C) and weighed to a constant mass. The weight loss was calculated by formula 1, where m_i—the sample weight after 1, 3, 7, and 14 days and 1, 2, and 3 months of incubation (g) and m_0—the sample weight before the test (g). The results are the arithmetic average of six measurements. In case of the PBS study, the pH solution was controlled every 2 weeks with the use of Metler Toledo pH-meter:

$$S = \left(\frac{m_i - m_0}{m_0}\right) \times 100\%. \quad (1)$$

Contact angle

Static contact angle of the fabricated PPS and native PUR was determined at room temperature with the use of Reichert Wien optical microscope (35× magnification). PPS and native PUR were cut into 2 cm^2 samples and its surface was purified with *n*-hexane (POCH, Poland) before the measurement. To determine the contact angle, the sessile drop method (SDM) was applied, using 5 μL of distilled water droplet. For each angle reported, at least ten measurements on different surface locations were averaged. The width and the height of the sessile drop were measured and the contact angle was determined. Literature data require polymeric materials of contact angle in the range of 45–76 as most suitable for cell adhesion and proliferation [32].

Mechanical properties

Tensile strength (T_{Sb}) and elongation at break (ε_b) of the fabricated PPS and native PUR were studied with the use of Zwick and Roell Z020 testing machine according to PN-EN ISO 527-1:2012. The crosshead speed was 50 ± 5 mm/min. The measurement was performed at room temperature. Six samples of PPS and native PUR were studied and the average values of T_{Sb} and ε_b presented.

Scanning electron microscopy (SEM)

SEM was performed for fabricated PPS with the use of SEM Zeiss EVO-40 microscope. Samples were gold-coated before analysis. Pore sizes were calculated from SEM images by Image J software (U.S. National Institutes of Healt, Bethesda, MA, USA). The average pore size was obtained by measuring the diameter of 100 pores chosen randomly throughout the central section of the samples. To perform statistical analysis of the pore size, we used Shapiro–Wilk test ($p < 0.05$) to determine the normal distribution of the data, and for the average pore size we used normal Gaussian–Lorentz distribution analysis. The scaffold porosity was

determined by using a liquid displacement method. Ethanol was used as the displacement liquid because it penetrates easily into the pores and does not induce shrinkage or swelling as a non-solvent of the polymers. A scaffold sample was immersed in a cylinder containing a known volume of ethanol (V_1). The sample was kept in ethanol for 5 min and then pressed to force air from the scaffold and allow the ethanol to penetrate and fill the pores. The total volume of ethanol and the ethanol-impregnated scaffold was recorded as V_2. The ethanol-impregnated scaffold was removed from the cylinder and the residual ethanol volume was recorded as V_3. The porosity of the scaffold was expressed as: $p = (V_1 - V_3)/(V_2 - V_3)$.

Microbiological studies

Microorganisms

Bacterial strains were cultivated in freshly autoclaved LB medium (10.0 g/L tryptone, 5.0 g/L yeast extract, and 10.0 g/L NaCl) at 37 °C for 24 h. After incubation, 200 μL of each bacterial strain culture was transferred as an inoculum into 100 mL sterile Erlenmeyer flasks containing 10 mL of the fresh LB medium. All analyzed bacterial strains were cultivated at 37 °C on a rotator shaker of 170 rpm speed to get the log phase. For determination of potential antibacterial activities of fabricated PPS, 100 μL of each bacterial strain in log phase was transferred and spread on LA plates (LA medium: 10.0 g/L, tryptone 5.0 g/L yeast extract, 10.0 g/L NaCl and 15 g/L agar) with a sterile glass rod. Afterward, the sterile samples of the examined PPS material were exposed to UV radiation for 30 min. Sterile samples were dried out in Thermobalance (RADWAG MAX 50/SX) set at 80 °C for 30 min and then placed with sterile tweezers on LA plates. Plates were incubated at 37 °C for 24 h. After the incubation, the presence or absence of zones of bacterial growth inhibition around PPS samples was observed. At the same time, the ability of *E. coli*, *S. aureus*, and *P. aeruginosa* cell adhesion and growth on PPS surface were studied. Sterile samples of PPS were placed in triplicate on two layers of growth medium. The bottom layer (solid layer) consisted of 0.8% agar solution. The top layer (liquid layer) consisted of modified PBS (phosphate-buffered saline). The modified PBS medium containing (g/L) NaCl 8.0; KCl 0.2; Na_2HPO_4 1.44; KH_2PO_4 0.24; $(NH_4)_2SO_4$ 0.2; agar 3.0 was dissolved in 1 L of deionized water, pH was adjusted to 7.4, and then the resulting medium was autoclaved (121 °C, 1–5 atm., 20 min) and cooled to room temperature. Sterile samples of PPS were placed on 0.8% agar surface and then poured into bacterial suspensions with the final concentration of CFU/mL around ~106 in modified PBS. The TOP surface of each analyzed PPS sample was covered with bacterial suspension. Petri plates with two-layer growth medium and analyzed PPS samples were incubated at 37 °C for 24 h, and 1 and 2 weeks. PPS samples after each time point were removed from LA plates with the use of sterile tweezers and transferred directly to 2.5% glutaraldehyde for 30 min. After that, the PPS samples were washed twice with PBS (containing, g/L: NaCl 8.0; KCl 0.2; Na_2HPO_4 1.44; KH_2PO_4) and twice distilled

water. The samples were dried in a Thermobalance set at 37 °C overnight and studied with the use of scanning electron microscope.

In vitro cytocompatibility studies

Indirect MTT cytotoxicity assay

The biocompatibility of the obtained PPS was studied in a in vitro test with the use of an indirect cytotoxicity test performed according to ISO 10993-5 standard. In this case, the MTT assay was carried out. The extracts of PPS were prepared and then had contact with 3T3 cells cultured in supplemented medium [33–35]. To obtain the extracts, sterile PPS samples were incubated in cell culture medium (Dulbecco's modified Eagle's medium, DMEM, supplemented with fetal bovine serum, FBS, and antibiotics) for 5 days at 37 °C. The ratio of the total surface area of samples to the volume of extraction medium was 3 cm^2/mL. DMEM supplemented with FBS and antibiotics was used as a negative, nontoxic, control. To determine cell viability, the colorimetric MTT metabolic activity assay was used. MTT was performed in three time points: 24, 48, and 72 h. Each day of the test, the MTT was added (0.5 mL) to the wells and incubated for 3 h at 37 °C. After that, the insoluble formazan crystals formed were dissolved using 2 mL of dimethylsulfoxide (DMSO, Sigma D2650 tissue culture grade) and optical densities were measured at a test wavelength of 570 nm in a Cecil CE 2021 spectrometer. The results were presented as reduction of metabolic activity in comparison to control cells cultured in the medium (100%). All assays were performed in triplicate.

Statistical analysis

Statistical analysis was performed with the use of the Origin Pro 8.5. To evaluate the statistical differences, two-way ANOVA ($\alpha = 0.05$) and post hoc Tukey test ($\alpha = 0.05$) were used.

Cell morphology

Cell morphology was monitored with the use of an inverted microscope (Nikon Eclipse TS 100, Japan) for each day of the MTT assay.

Results

Fourier transform infrared spectroscopy (FTIR)

The FTIR spectra of fabricated PPS and native PUR are presented in Fig. 4. Due to FTIR analysis, the presence of functional groups, characteristic for native PUR materials, was confirmed in PPS as well (Fig. 4). The weak absorption peak, observed at 3319 cm^{-1}, was assigned to stretching vibrations of NH groups, which

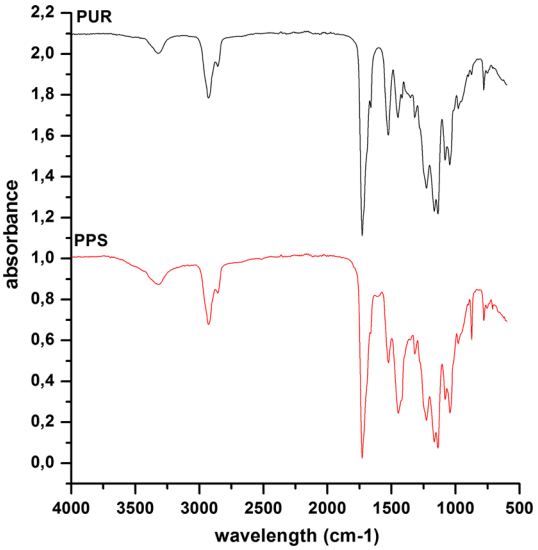

Fig. 4 FTIR spectra of fabricated PPS and active PUR

were present in both native PUR materials and fabricated PPS. The broad peak of NH stretching was related to the hydrogen bonds present in the chemical structure of native PUR and PPS. The observed asymmetric and symmetric stretching vibrations of CH_2 groups were noted between 2930 and 2854 cm^{-1} in both cases of the studied materials. Very strong carbonyl stretching peak appeared at 1726 cm^{-1} and it was directly related to the presence of a substantial amount of non-hydrogen-bonded or poorly organized hydrogen-bonded carbonyl urethane groups. On the other hand, at 1655 cm^{-1} a peak was observed, which was related to ordered and strongly hydrogen-bonded urethane groups in native PUR and was present in fabricated PPS as well [36]. The peak noted at 1527 cm^{-1} was related to the NH group deformation vibrations. Signals indicated in the range of 1451–1314 cm^{-1} were with respect to the planar vibrations of the symmetric and asymmetric CH_2 groups. The peaks observed at 1221–1217 cm^{-1} are related to the N–C stretching of the urethane bonding present in native PUR and confirmed as well in fabricated PPS. The peaks at 1168, 1138, 1164, and 1129 cm^{-1}, respectively, for native PUR and fabricated PPS, correspond to the CO–O stretching of ester groups of dHEBA, and peaks in the range 969–779 cm^{-1} are related to out-of-plane bonding vibrations of C–H bending, CH_2 scissoring, CH_2 wagging, and NH and OH scissoring and wagging. FTIR studies showed that the used fabrication technique did not influence the chemical composition of fabricated PPS in comparison to native PUR. That may also suggest that thermal degradation of PUR during PPS fabrication was not observed.

Proton nuclear magnetic resonance (HNMR)

The HNMR spectra of fabricated PPSs and native PUR are presented in Fig. 5. The HNMR spectra confirmed the presence of urethane bonds in the studied native PUR materials as well as in fabricated PPS (Fig. 5). Both proton signals of soft and hard

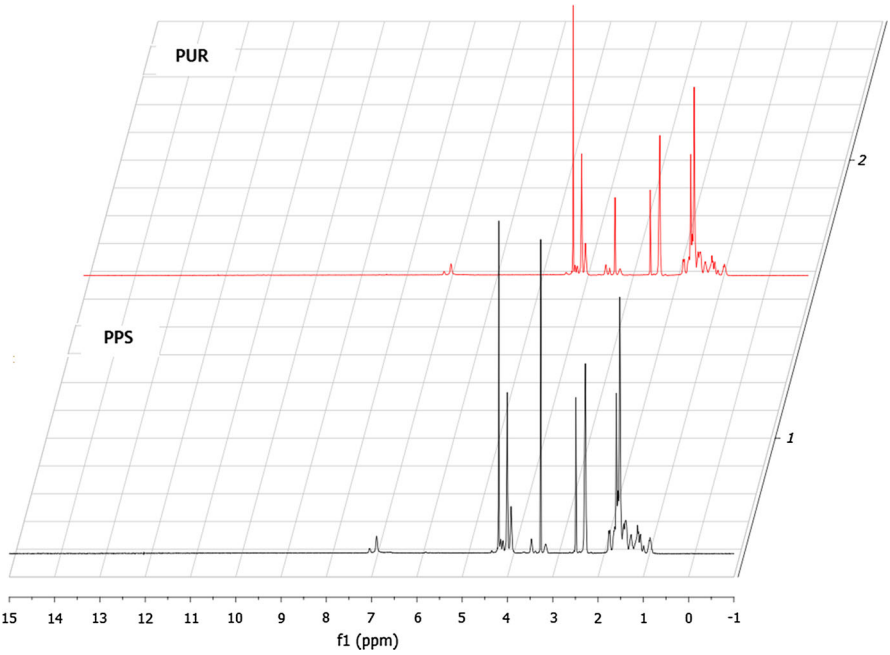

Fig. 5 The HNMR spectra of native PUR and fabricated PPS

segments were confirmed. Proton signals detected between 0.5 and 1 ppm were related to the protons of aliphatic CH_2 groups located in the middle of the PUR chain in the direct neighborhood of other aliphatic origin protons (CH_2 groups). In the range of 1–1.5 ppm, protons of aliphatic CH_2 groups were indicated in the soft and hard segments of polyurethane structure closer to electron-withdrawing groups (EWG) like –CO–O– and –O–. the protons noted between 1.5 and 2.2 ppm were considered as aliphatic CH_2 groups present in polyester dHEBA in the closest neighborhood of C=O (β position). At 2.5 ppm, the DMSOd6 solvent was recognized. Protons indicated in the range of 3–3.5 ppm were related to CH_2 groups in the closest neighborhood with –NH–CO–O– urethane bonds at the NH side. At 4.0 ppm, protons of aliphatic CH_2 groups were recognized in polyester –CO–O– groups in the close neighborhood of –O–. Protons of NH groups, which form intermolecular hydrogen bondings in native PUR or PPS structure, were detected between 6.5 and 7.5 ppm. The HNMR spectra confirmed the formation of polyurethane. The procedure of PPS fabrication did not disturb the chemical urethane structure of the obtained PPS.

Differential scanning calorimetry (DSC) and transmission electron microscopy (TEM)

Figure 6 presents the DSC curves-fabricated PPS and native PUR. The DSC results of only one heating cycle are presented. Figure 7 shows the TEM micrographs of fabricated PPS and native PUR. The DSC study did not show significant changes in

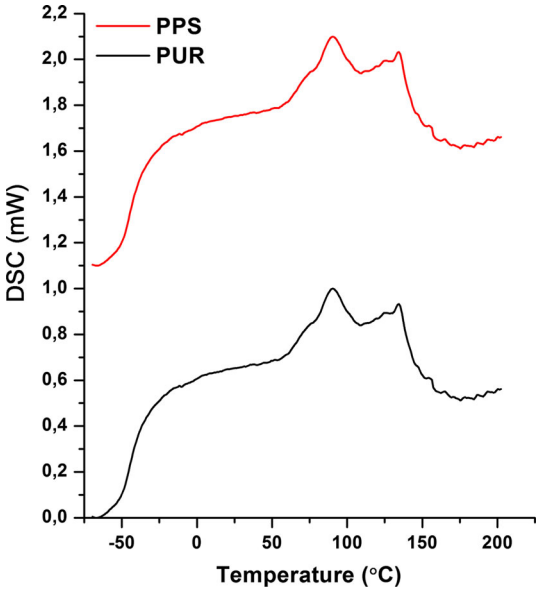

Fig. 6 DSC curves of fabricated PPS and native PUR

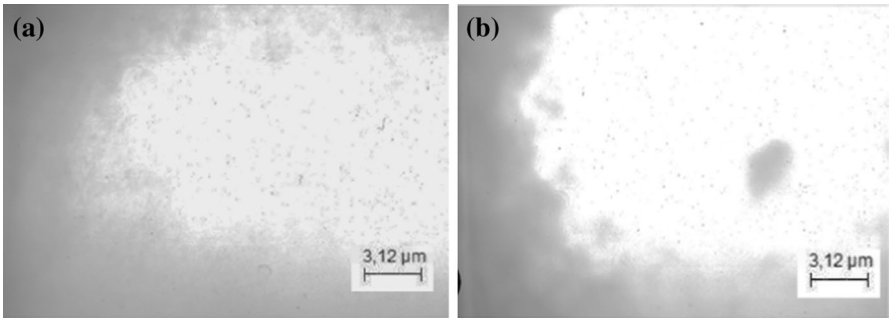

Fig. 7 TEM micrographs of **a** fabricated PPS and **b** native PUR viewed at magnification ×3000

the glass transition temperature (T_g) of fabricated PPS and native PUR, which was noticed around −38 °C (Fig. 6). Two melting points were observed in both PPS and native PUR cases. The first melting peak was indicated at 92 °C and the second at 135 °C. This suggests a two-phase structure of fabricated PPS and native PUR. The two-phase morphology of both fabricated PPS and native PUR was confirmed by TEM analysis, which revealed the presence of the distinguished matrix phase and dispersed phase that were mutually immiscible (Fig. 7).

Interactions with canola oil, distilled water, saline, and phosphate-buffered saline

Interactions with media were studied for both fabricated PPS and native PUR. The results of the performed studies are presented in Fig. 8. Canola oil sorption, which

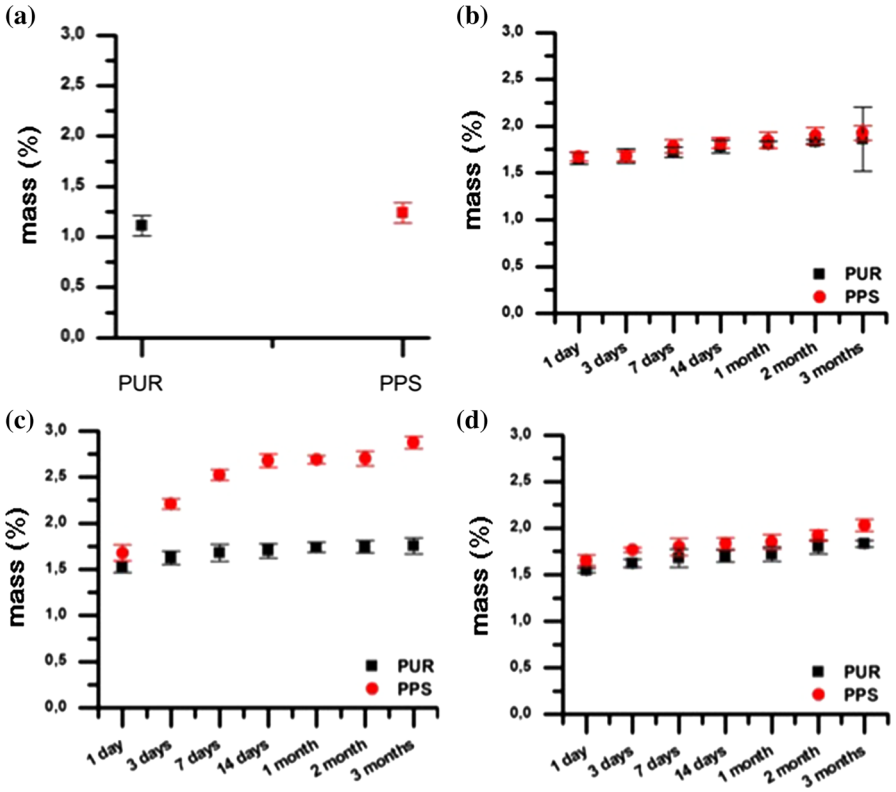

Fig. 8 Interactions of fabricated PPS and native PUR with: **a** canola oil, **b** water, **c** saline solution, **d** PBS

value was in the range of 1.0–1.5%, was comparable for fabricated PPS and native PUR (Fig. 8). The sorption of distilled water (1.5–2.0%) was similar as well for both types of studied materials. The values of saline sorption were in the range of 1.75–3.0% for fabricated PPS and 1.5–1.75% for native PUR. In case of PBS sorption, the obtained values were in the range of 1.5–2.0% for both fabricated PPS and native PUR. The fabricated PPS as well as native PUR were stable in the studied media during 3 months of incubation. pH was controlled every 2 weeks and did not differ between samples; it was in the range of 7.4–7.6.

Scanning electron microcopy (SEM)

SEM was performed for fabricated PPS to determine their morphology. The SEM micrograph of the obtained PPS is presented in Fig. 9. PPS obtained by combined SC/PL with TIPS technique was highly porous—87% (Fig. 9). A pore size of PPS was in the range of 98–329 μm, and an average scaffold pore size was 154 ± 2 μm.

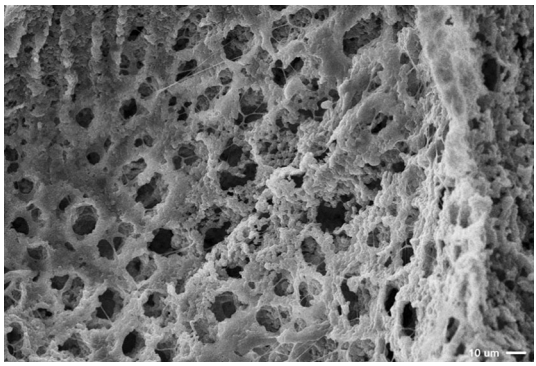

Fig. 9 Selected SEM micrograph of PPS morphology

Table 1 Mechanical properties of fabricated PPS and native PUR

Symbol	T_{Sb} (MPa)	ε_b (%)
PUR	1.2 ± 0.7	144 ± 8
PPS	0.654 ± 0.9	95 ± 10

Table 2 Contact angle of the obtained PUR materials and fabricated PPS

Symbol	Water contact angle (average ± SD°)
PUR	68 ± 4
PPS	54 ± 3

Mechanical properties of unmodified and AA-modified PPS

Table 1 presents the tensile strength and elongation at break of fabricated PPS and native PUR.

The tensile strength (T_{Sb}) and percent of elongation at break (ε_b) (Table 1) of native PUR materials (1.2 ± 0.7 MPa) were higher than for fabricated PPS (0.654 ± 0.9 MPa). The percent of elongation at break was higher as well for native PUR materials (144 ± 8%) in comparison to PPS (95 ± 10%). The fabrication of native PUR materials into PPS significantly influenced the mechanical properties and caused their decrease.

Contact angle

The contact angles of fabricated PPS and native PUR are presented in Table 2. The contact angle of fabricated PPS (54° ± 3°) was slightly lower than native PUR (68° ± 4°). The fabrication procedure influenced the contact angle of the produced scaffolds (Table 2).

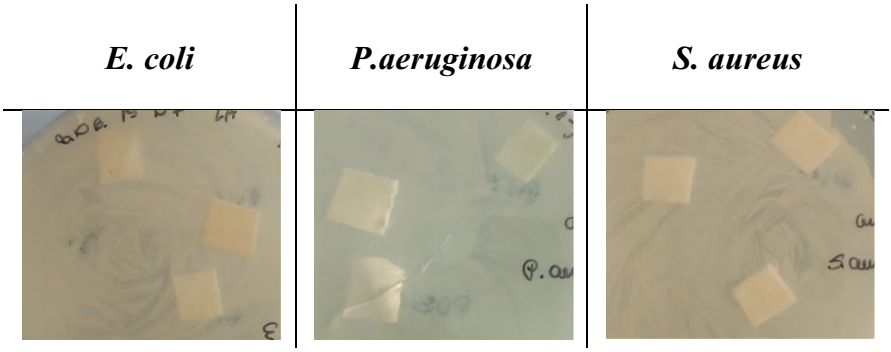

Fig. 10 Absence of inhibition zones in performed DDA with the use of PPS on bacterial species *E. coli*, *P. aeruginosa*, and *S. aureus*

Microbiology

Disc diffusion assay

Figure 10 shows the results of disc diffusion assay, which was performed on fabricated PPS to determine the presence or absence of antimicrobial properties of PPS. The results of culturing of *E. coli*, *P. aeruginosa*, and *S. aureus* in the presence of PPS revealed the lack of the antimicrobial effect on the analyzed bacterial species (Fig. 10). In a parallel study, we analyzed the ability of bacterial cells for adhesion and growth on PPS surface. After 2 weeks of bacterial species cultivation in the presence of PPS, the adhesion and growth of *E. coli* and *S. aureus* cells were observed inside the pores of the analyzed material (Fig. 11). Unfortunately, we did not find the presence of *P. aeruginosa* on the PPS surface. To summarize, the absence of inhibition zones around the PPS scaffold and *E. coli* and *S. aureus* adhesion to the PPS scaffold surface indicate that the PPS scaffold seems to be nontoxic to the cells of the studied bacterial cultures. Moreover, PPS provided good substrate for microorganism growth, which were well adhered to the PPS surface (Fig. 11). After 2 weeks of bacterial species growth, the formation of colonies was observed (marked with red circles in Fig. 11).On the other hand, the absence of inhibition zones around the PPS and good bacterial species adhesion to the PPS surface indicate that the PPS scaffold seems to be not toxic to the cells of the studied bacterial cultures.

In vitro cytocompatibility studies

Indirect MTT cytotoxicity assay

The results of the performed MTT assay are presented in Fig. 12. From Fig. 12, it can be concluded that PPS were more biocompatible than native PUR. They revealed moderate cytotoxic effect on 3T3 fibroblast cells. It was recognized that

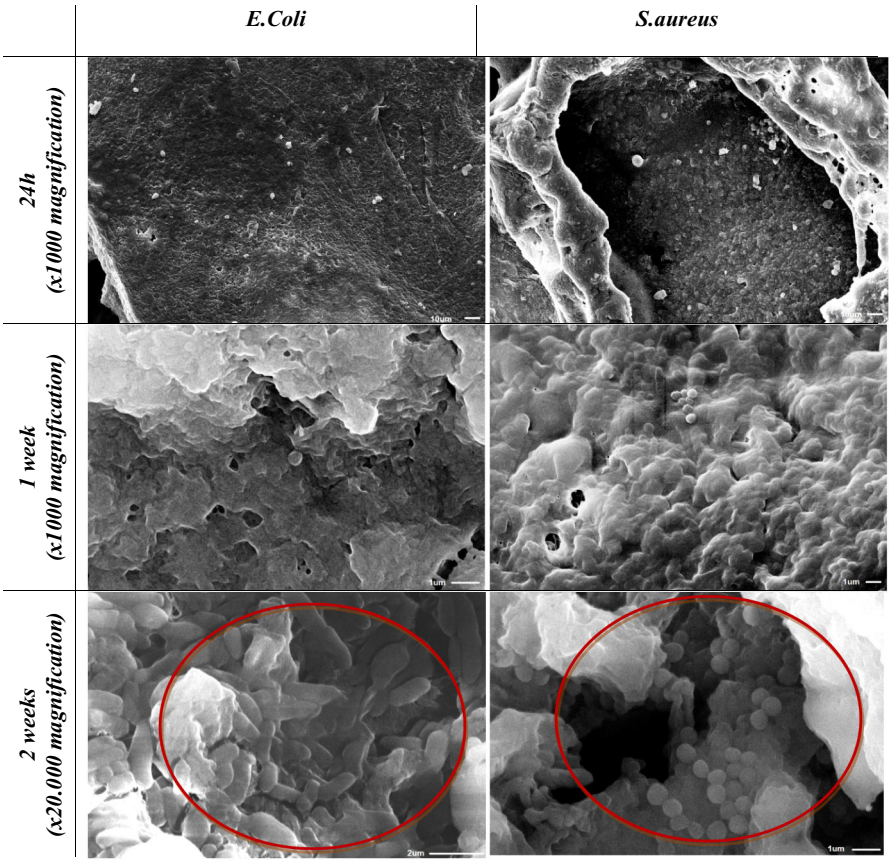

Fig. 11 Bacterial species (*E. coli* and *S. aureus*) adhesion to the PPS surface after 24 h, and 1 and 2 weeks of culture

PPS after each time point (24, 48 and 72 h) had higher cell viability (67 ± 2%, 40 ± 1% and 18 ± 1%, respectively) in comparison to native PUR (24 h-12 ± 1%, 48 h-7 ± 1% and 72 h-3 ± 1%). Native PUR materials appeared to be severely toxic to 3T3 cells.

Cell morphology

Cell morphology is presented in Fig. 13. From Fig. 13, it can be observed that 3T3 cells, which had contact with PPS extracts, had morphology comparable to the control up to 48 h of incubation. After the 72 h time point, large detachment of cell from the well was observed. In case of PUR materials observed, cell morphology was not comparable to the controls from the first time point of the MTT assay (24 h). Cell morphology was violated. Moreover, cells not attached to the well were diluted in the culturing medium. After 72 h, cells were degenerated in their shape.

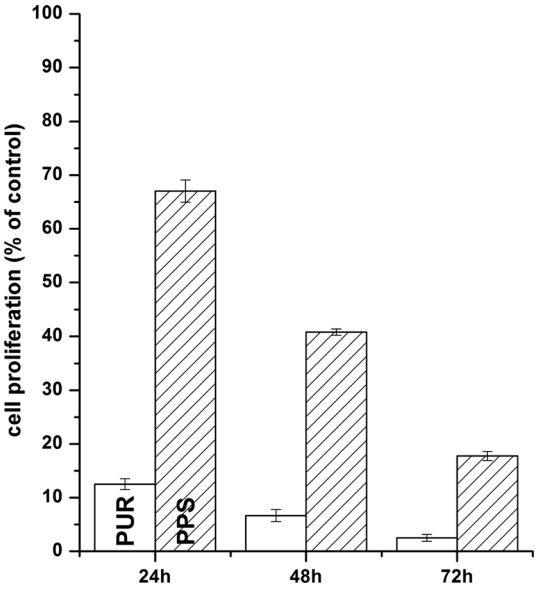

Fig. 12 The effect of fabricated PPS and native PUR extracts on the in vitro growth of mouse fibroblast 3T3 cells measured using MTT assay after 24, 48, and 72 h (*$p < 0.05$)

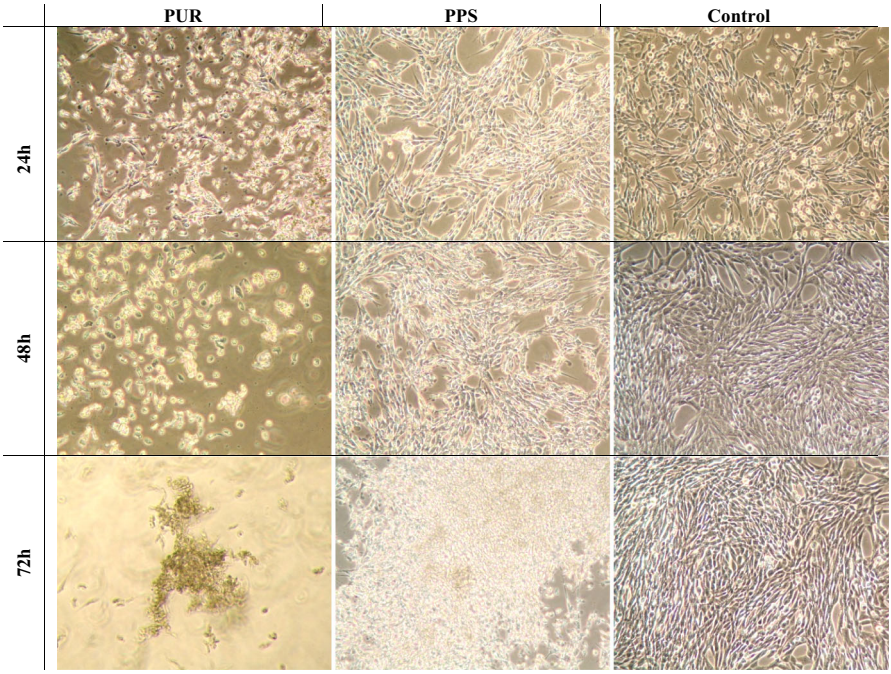

Fig. 13 Changes of 3T3 cell morphology during the MTT assay

Statistical analysis revealed significant influence of processing technique on 3T3 cells viability at each time point of the performed test.

Discussion

The effort to develop tissue-implantable construction is one of the most demanding and challenging applications of tissue engineering, because soft tissues such as myocardium, blood vessels, skeletal muscle, adipose tissue, and even cartilage often possess large volumes, have high cell densities, and can be mechanically active [37, 38]. In this study we have synthesized native PUR, which was fabricated into the PPS by SC/PL combined with TIPS technique for regenerative medicine of soft tissues. The performed FTIR studies showed that the PPS fabrication technique used in this study, combined SC/PL with TIPS, did not influence the chemical composition of the obtained PPS in comparison to native PUR. Chemical functional groups present in native PUR materials were indentified in fabricated PPS as well. That may suggest that the degradation of the native PUR material, subjected to fabrication into PPS, did not occur. The HNMR spectra confirmed the formation of polyurethane chemical structure and hydrogen bonds. The presence of urethane linkage as well as soft and hard segments in both fabricated PPS and native PUR was confirmed. The protocol of PPS fabrication did not disturb the chemical structure of the obtained PPS. The DSC study did not show significant changes in the glass transition temperature (T_g) of fabricated PPS in comparison to the native PUR. T_g was noticed around −38 °C for both of the studied materials. The two melting points (92 and 135 °C) observed were related to PPS and native PUR structural phase separation, which was confirmed by TEM analysis. The presence of immiscible dispersed phase and matrix phase in fabricated PPS and native PUR may be related to the used HMDI diisocyanate, which is a mixture of isomers (cis–cis, trans–trans, trans–cis) of different reactivities [22, 39–41]. Interaction studies of fabricated PPS and native PUR with selected media: canola oil, distilled water, saline, and PBS did not reveal degradation progress during the 3 months study. The examined PPS and native PUR were stable and suitable for tissue engineering applications, due to the fact that there is a possibility of controlling the degradation rate of the obtained PPS, which should match the rate of tissue growth in vitro and in vivo [5]. Literature reports that the degree of degradation has to be controlled in such a way that the scaffold retains its physicochemical and mechanical properties for at least 3–6 months. During 1–3 months, cells are constantly proliferating and between 3 and 6 months regeneration occurs in situ. Henceforth, the scaffold matrix may start losing its mechanical properties and should be metabolized by the body without foreign body reaction after 12–18 months [42–45]. The studied pH did not change significantly during 3 months of sample incubation and it was in the range of 7.4–7.6.

PPS obtained by combined SC/PL with TIPS technique was highly porous—87%. Such porosity meets the requirements of polymeric scaffolds for tissue engineering applications [1], due to the fact that the highly porous structure of the scaffold with an open fully interconnected geometry and provided large surface area

allows for cell ingrowths and uniform distribution as well as facilitates the neovascularization of the construct [46]. The pore size of the fabricated PPS was in the range of 98–329 μm and the average scaffold pore size was 154 ± 2 μm. Pore size is a very important factor. When pores are too small, they will cause occlusion by the cells, which will prevent cellular penetration, extracellular matrix production, and neovascularization of the inner areas of the scaffold. The effects of pore size on tissue regeneration have been emphasized by experiments demonstrating optimum pore size of 5 μm for neovascularization [47], 5–15 μm for fibroblast ingrowth [48], 20 μm for the ingrowth of hepatocytes [49], 200–350 μm for osteoconduction [50], and 20–125 μm for regeneration of adult mammalian skin [51]. Pore interconnectivity is critical to ensure that all cells are within 200 μm from the blood supply to provide for mass transfer of oxygen and nutrients [52]. The proper mechanical properties for a biomaterial to be used in a tissue engineering application are critical to the success of the implant. The biostability of many scaffolds depends on the factors such as strength, elasticity, and absorption at the material interface and its chemical degradation [53]. The mechanical properties of bulk biomaterials are altered by their processing into scaffolds of various pore sizes and pore orientations and further these properties will rapidly diminish as a function of implantation time [54]. The mechanical rigidity of the surrounding matrix, as well as material roughness and physical confinement, may significantly modulate the outcome of the balance between cell–cell forces and intracellular signaling [55–57]. The major factor affecting the mechanical properties and structural integrity of scaffolds, however, is their porosity; for example, pore volume, size, shape, orientation, and connectivity. The mechanical properties of the obtained PPS were satisfactory for tissue engineering purpose. The tensile strength and percent elongation at break of the fabricated PPS ($T_{Sb} = 0.654 \pm 0.9$ MPa, $\varepsilon_b = 95 \pm 10\%$ respectively) were comparable to the native soft tissues, e.g., aorta: $T_{Sb} = 0.3$–0.8 MPa, $\varepsilon_b = 50$–100% [58–60]. Due to this fact, the obtained PPS might be considered as a solution applicable in the field of regenerative medicine. It is worth mentioning that the fabrication of PUR materials into PPS significantly influences the mechanical properties and causes their decrease of 55% in the case of tensile strength and 66% in the case of elongation at break. Such possible changes in the mechanical properties in the processing of cast PUR into PPS should be taken into account while designing the final PPS product. On the other hand, the obtained decreased mechanical properties of PPS are more suitable for soft tissue engineering applications [58–60]. The contact angle of fabricated PPS (54° ± 3°) slightly decreased in comparison to native PUR (68° ± 4°). Contact angle study revealed that the obtained PPS were hydrophilic and suitable for mammalian cells culturing on the polymeric surface according to literature references, which report the range of the most suitable contact angle of 45°–76° for mammalian cell growth and proliferation. This is also related to the possibility of hydrophilic materials to form more hydrogen bonds, which improves the biocompatibility of polymeric materials by solvation of water molecules, which form a biologically neutral water film at the surface [32]. It was reported that the low values of the contact angle results in improved biocompatibility [61, 62].

The microbiological studies performed did not reveal the presence of antimicrobial effect on the analyzed bacterial species which is comparable to the literature reports [63]. On the other hand, the absence of inhibition zones around PPS and good bacterial species adhesion to the PPS surface indicate that the PPS scaffold seems to be not toxic to the cells of the studied bacterial cultures. To evaluate the biocompatibility of the obtained PPS, the MTT cytotoxicity test was performed. The obtained PPS were more biocompatible than the PUR materials. It could be caused by better material purification and short polyurethane chain removal, which might have occurred during the PPS fabrication protocol [64]. 3T3 cells, which had contact with PPS extracts, had morphology comparable to control up to 48 h of incubation. After the 72 h time point, a large detachment of cells from the well was observed. In case of PUR materials, the observed cell morphology was not comparable to the controls from the first time point of the MTT assay (24 h). The cell morphology was violated. Moreover, cells not attached to the well were diluted in the culturing medium. After 72 h, shape degeneration of cells occurred. Statistical analysis revealed significant influence of processing technique on 3T3 cell viability at each time point of this test. This may confirm the better purification of PPS related to removal of short chains of polyurethane during the fabrication protocol [64, 65].

Conclusions

In this study, we successfully fabricated porous polyurethane scaffolds (PPS) with the use of SC/PL combined with the TIPS technique. The performed FTIR and HNMR analyses confirmed the presence of chemical functional groups and chemical structure characteristics for polyurethane materials, which means that the processing of native PUR into PPS did not influence its chemical composition. The DSC analysis did not reveal changes in glass transition temperature between PUR materials and PPS (−38 °C), but it showed two melting points at 92 and 135 °C, which were related to their microstructure phase separation confirmed by TEM studies. The observed phase separation was finally related to the presence of HMDI isomers of different reactivities, which influence strongly the PPS and native PUR microstructure properties such as homogeneity. The study of PPS interactions with selected media (canola oil, distilled water, saline solution, and PBS) did not reveal significant changes in the mass loss of the obtained materials confirming at the same time that the obtained PPS were stable during the 3 months of incubation. On the other hand, significant improvement in the hydrophilic behavior of the studied samples as well as mechanical properties was indicated after processing PUR materials into PPSs (a contact angle decrease from 68° ± 4° to 54° ± 3° and mechanical properties from $T_{Sb} = 1.2 \pm 0.7$ MPa, $\varepsilon_b = 144 \pm 8\%$ to $T_{Sb} = 0.654 \pm 0.9$ MPa, $\varepsilon_b = 95 \pm 10\%$). The porosity of the scaffold was highly satisfactory (87%) and the pore sizes were suitable for soft tissue engineering purpose (98–329 μm and average pore size 154 ± 2 μm). Microbiological studies did not show inhibition zones around PPS, but on the other hand the absence of inhibition zones around PPS and good bacterial species adhesion to the PPS surface

indicated that the PPS scaffold seemed not to be toxic to the cells of the studied bacterial cultures. The performed cell studies revealed that the obtained PPS were more biocompatible than PUR materials, which might be related to PPS purification of the short chains that might have occurred during the PPS fabrication protocol. The fabricated PPS might be a useful tool in soft tissue engineering applications such as blood vessel reconstruction.

References

1. Dhandayuthapani B, Yoshida Y, Maekawa T, Kumar DS (2011) Polymeric scaffolds in tissue engineering application: a review. Int J Polym Sci Article ID 290602, p 19
2. Langer R, Vacanti JP (1993) Tissue engineering. Science 260(5110):920–926
3. Langer R, Tirell DA (2004) Designing materials for biology and medicine. Nature 428(6982):487–492
4. Fuchs JR, Nasseri BA, Vacanti JP (2001) Tissue engineering: a 21st century solution to surgical reconstruction. Ann Thorac Surg 72(2):577–591
5. Ramakrishna S, Mayer J, Wintermantel E, Leong KW (2001) Biomedical applications of polymer-composite materials: a review. Compos Sci Technol 61(9):1189–1224
6. Vert M (2005) Aliphatic polyesters: great degradable polymers that cannot do everything. Biomacromol 6(2):538–546
7. Piskin E (1994) Biodegradable polymers as biomaterials. J Biomater Sci Polym Ed 6:775–795
8. Ji Y, Ghosh K, Shu XZ, Li B, Sokolov JC, Prestwich GD et al (2006) Electrospun three-dimensional hyaluronic acid nanofibrous scaffolds. Biomaterials 27(20):3782–3792
9. Guntaillake P, Mayadunne R, Adhikari R (2006) Recent developments in biodegradable synthetic polymers. Biotechnol Ann Rev 12:301–347
10. Ma PX (2004) Scaffolds for tissue fabrication. Mater Today 7(5):30–40
11. Kucinska-Lipka J, Gubanska I, Janik H (2013) Polyurethanes modified with natural polymers for medical application. Part I. Polyurethane/chitosan and polyurethane/collagen. Polim (Polym) 58(9):678
12. Kucinska-Lipka J, Gubanska I, Janik H (2014) Polyurethanes modified with natural polymers for medical application. Part II. Polyurethane/gelatin, polyurethane/starch, polyurethane/cellulose. Polim (Polym) 3:195
13. Kucinska-Lipka J, Gubanska I, Janik H (2013) Gelatin-modified polyurethanes for soft tissue scaffold. Sci World J Article ID 450132, p 12
14. Guelcher SA (2008) Biodegradable polyurethanes: synthesis and applications in regenerative medicine. Tissue Eng Part B 14(1):3–17
15. Kucinska-Lipka J, Gubanska I, Janik H, Sienkiewicz M (2015) Fabrication of polyurethane and polyurethane based composite fibers by the electrospinning technique for soft tissue engineering of cardiovascular system. Mater Sci Eng C 46:166–176
16. Ma PX, Zhang R (2001) Microtubular architecture of biodegradable polymer scaffolds. J Biomed Mater Res 56(4):169–477
17. Hutmacher DW (2001) Scaffold design and fabrication technologies for engineering tissues—state of the art and future perspectives. J Biomater Sci 12(1):107
18. Freed LE, Vunjak-Novakovic G (1998) Culture of organized cell communities. Adv Drug Deliv Rev 33(1–2):15–30
19. Janik H, Marzec M (2015) A review: fabrication of porous polyurethane scaffolds. Mater Sci Eng C Mater Biol Appl 48:586–591
20. Vasita R, Katti DS (2006) Nanofibers and their applications in tissue engineering. Int J Nanomed 1(1):15–30
21. Sokolsky-Papkov M, Aghashi K, Olaye A, Shakesheff K, Domb AJ (2007) Polymer carriers for drug delivery in tissue engineering. Adv Drug Deliv Rev 59(4–5):187–206

22. Seneker SD, Born L, Schmelzer HG, Eisenbach CD, Foscher K (1992) Diisocyanato dicyclohexylmethane: structure/property relationships of its geometrical isomers in polyurethane elastomers. Colloid Polym Sci 270(6):553
23. Kucinska-Lipka J, Gubanska I, Janik H, Pokrywczynska M, Drewa T (2015) L-ascorbic acid modified poly(ester urethane)s as a suitable candidates for soft tissue engineering applications. React Funct Polym 97:105–115
24. Silvestri A, Boffito M, Sartori S, Ciardelli G (2013) Biomimetic materials and scaffolds for myocardial tissue regeneration. Macromol Biosci 13:984–1019
25. Boffito M, Sartori S, Ciardelli G (2014) Polymeric scaffolds for cardiac tissue engineering: requirements and fabrication technologies. Polym Int Forthcom 63:2–11
26. Janik H, Marzec M (2015) A review: fabrication of porous polyurethane scaffolds. Mater Sci Eng C 48:586–591
27. Janik H (2005) Struktury nadcząsteczkowe i wybrane właściwości rozgałęzionych i usieciowanych poli(estro-uretanów), poli(etero-uretanów) i poli(uretano-biuretanów) formowanych reaktywnie. Zeszyty Naukowe Politechniki Gdańskiej
28. Szelest-Lewandowska A (2003) Novel polyurethanes for medical applications. PhD Thesis, Gdansk University of Technology, Gdansk
29. Brzeska J, Heimowska A, Sikorska W, Jasińska-Walc L, Kowalczuk M, Rutkowska M (2015) Chemical and enzymatic hydrolysis of polyurethane/polylactide blends. Int J Polym Sci 2015:795985
30. Roeder RK (2013) Mechanical characterization of biomaterials. In: Bandyopadhyay A, Bose S (eds) Characterization of biomaterials, chap 3. Elsevier, p 94
31. Wei L, Li G, Yan YD, Pradhan R, Kim JO, Quan Q (2012) Lipid emulsions as a drug delivery system for breviscapine: formulation development and optimization. Arch Pharm Res 35(6):1037–1043
32. Guelcher SA, Srinivasan A, Dumas JE, Didier JE, McBride S, Hollinger JO (2008) Synthesis, mechanical properties, biocompatibility and degradation of polyurethane networks from lysine polyisocyanates. Biomaterials 29:1762–1775
33. Cetina-Diaz SM, Chan-Chan LH, Vargas-Coronado RF, Cervantes-Uc JM, Quintana-Owen P (2014) Physicochemical characterization of segmented polyurethanes prepared with glutamine or ascorbic acid as chain extenders and their hydroxyapatite composites. J Mater Chem B 2:1966
34. Punnakitikashem P, Truong D, Menon JU, Nguyen KT, Hong Y (2014) Electrospun biodegradable elastic polyurethane scaffolds with dipyridamole release for small diameter vascular grafts. Acta Biomater 10:4618–4628
35. Nair PA, Ramesh P (2013) Electrospun biodegradable calcium containing poly(ester urethane) urea: synthesis, fabrication, in vitro degradation and biocompatybility evaluation. J Biomed Mater Res Part A 101:1876–1887
36. Yilgor I, Yilgor E, Guler IG, Ward TC, Wilkies GL (2006) FTIR investigation of the influence of diisocyanate symmetry on the morphology development in model segmented polyurethanes. Polymer 47:4105–4114
37. Guan J, Stankus JJ, Wagner WR (2006) Soft tissue scaffolds. Wiley Encyclopedia of Biomedical Engineering. Wiley-Interscience, US
38. Pokrywczynska M, Gubanska I, Drewa G, Drewa T (2015) Application of bladder acellular matrix in urinary bladder regeneration: the state of the art and future directions. Biomed Res Int 2015:613439
39. Lee DK, Tsai HB (2000) Properties of segmented polyurethanes derived from different diisocyanates. J Appl Polym Sci 75:167–174
40. Kanapitsas A, Pissis P, Ribelles G, Pradas M, Privalko EG, Privalko VP (1999) Molecular mobility and hydration properties of segmented polyurethanes with varying structure of soft and hard-chain segments. J Appl Polym Sci 71:1209–1221
41. Janik H (2010) Progress in the studies of the supermolecular structure of segmented polyurethanes. Polim (Polym) 6:419
42. Hutmacher DW (2008) Scaffold-based bone engineering by using rapid prototyping technologies in Virtual and Rapid manufacturing. In: Bartolo JB (ed) Advanced research in virtual and rapid prototyping. Taylor & Francis Group, New York, p 65
43. Middleton JC, Tipton AJ (2000) Synthetic biodegradable polymers as orthopedic devices. Biomaterials 21(23):2335–2346
44. Bose S, Roy M, Bandyopadhyay A (2012) Recent advances in bone tissue engineering scaffolds. Trend Biotechnol 30(10):546–554
45. Liu X, Chen W, Gustafson CT, Miller AL, Waletzki BE (2015) Tunable tissue scaffolds fabricated by in situ crosslink phase separation system. RSC Adv 5:100824

46. Leon CA, Leon Y (1998) New perspectives in mercury porosimetry. Adv Colloid Interface Sci 76–77:341–372
47. Brauker JH, Carr-Brendel VE, Martinson LA, Crudele J, Johnston WD, Johnson RC (1995) Neovascularization of synthetic membranes directed by membrane micro architecture. J Biomed Mater Res 29:1517–1524
48. Klawitter JJ, Hulbert SF (1971) application of porous ceramics for the attachment of load-bearing internal orthopedic applications. J Biomed Mater Res A Symp 2:161–168
49. Yang S, Leong KF, Du Z, Chua CK (2001) The design of scaffolds for use in tissue engineering—part I: traditional factors. Tissue Eng 7(6):679–689
50. Whang K, Healy KE, Elenz DR, Nam EK, Tsai DC, Thomas CH et al (1999) Engineering bone regeneration with bioabsorbable scaffolds with novel microarchitecture. Tissue Eng 5(1):35–51
51. Yannas IV, Lee E, Orgill DP, Skrabut EM, Murphy GF (1989) Synthesis and characterization of a model extracellular matrix that induces partial regeneration of adult mammalian skin. Proc Natl Acad Sci USA 86(3):933–937
52. Salgado AJ, Coutinho OP, Reis RL (2004) Bone tissue engineering: state of the art and future trends. Macromol Biosci 4(8):743–765
53. Nair LS, Laurencin CT (2007) Biodegradable polymers as biomaterials. Progr Polym Sci 32(8–9):762–798
54. Anseth KS, Bowman CN, Brannon-Peppas L (1996) Mechanical properties of hydrogels and their experimental determination. Biomaterials 17(17):1647–1657
55. Moghe PV, Berthiaume F, Ezzel RM, Toner M, Tompkins RG, Yarmush ML (1996) Culture matrix configuration and composition in the maintenance of hepatocyte polarity and function. Biomaterials 17(3):373–385
56. Rayan PL, Foty RA, Kohn J, Steinberg MS (2001) Tissue spreading on implantable substrates is a competitive outcome of cell–cell vs cell-substrate adhesivity. Proc Natl Acad Sci USA 98(8):4323–4327
57. Ingber DE (2002) Mechanical signalling and the cellular response to extracellular matrix in angiogenesis and cardiovascular physiology. Circ Res 91(10):877–887
58. Wagenseil JE, Mecham RP (2009) Vascular extracellular matrix and arterial mechanics. Physiol Rev 89(3):957–989
59. Holzapfel GA (2000) Biomechanics of soft tissue. Comput Biomech 7
60. Akhtar R, Sherratt MJ, Cruickshank JK, Derby B (2011) Characterizing the elastic properties of tissues. Mater Today 14(3):96–105
61. Han DK, Park KD, Ryu GH, Kim UY, Min BG, Kim YH (1996) Plasma protein adsorption to sulfonated poly(ethylene oxide)-grafted polyurethane surface. J Biomed Mater Res 30:23–30
62. Desai NP, Hubbel JA (1991) Biological responses to polyethylene oxide modified polyethylene terephthalate surfaces. J Biomed Mater Res 25:829–843
63. Morton LHG, Surman SB (1994) Biofilms in biodeterioration—a review. Int Biodeter Biodegr 32:203–221
64. Hoskins C, Cheng WP (2013) Hydrophobic drug solubilisation in Fundamentals of pharmaceutical nanoscience. In: Uchegbu I, Schatzlein AG, Cheng WP, Lalotsa A (eds) 14 edn, Springer, NY, p 386
65. Karchin A, Simonovsky FI, Ratner BD, Sanders JE (2011) Melt electrospinning of biodegradable polyurethane scaffolds. Acta Biomater 7(9):3277–3284